L. Zhu[1]
Department of Mechanical Engineering,
University of Maryland, Baltimore County,
Baltimore, MD 21250
e-mail: zliang@umbc.edu

M. Tolba
Department of Endodonics, Prosthodontics and
Operative Dentistry,
and Department of Health Promotion and Policy,
University of Maryland, Baltimore,
Baltimore, MD 21201

D. Arola
Department of Mechanical Engineering,
and Department of Endodonics, Prosthodontics
and Operative Dentistry,
University of Maryland, Baltimore County,
Baltimore, MD 21250

M. Salloum
Department of Mechanical Engineering,
University of Maryland, Baltimore County,
Baltimore, MD 21250

F. Meza
Department of Endodonics, Prosthodontics and
Operative Dentistry,
University of Maryland, Baltimore,
Baltimore, MD 21201

Evaluation of Effectiveness of Er,Cr:YSGG Laser For Root Canal Disinfection: Theoretical Simulation of Temperature Elevations in Root Dentin

Erbium, chromium: yttrium, scandium, gallium, garnet (Er,Cr:YSGG) lasers are currently being investigated for disinfecting the root canal system. Prior to using laser therapy, it is important to understand the temperature distribution and to assess thermal damage to the surrounding tissue. In this study, a theoretical simulation using the Pennes bioheat equation is conducted to evaluate how heat spreads from the canal surface using an Er,Cr:YSGG laser. Results of the investigation show that some of the proposed treatment protocols for killing bacteria in the deep dentin are ineffective, even for long heating durations. Based on the simulation, an alternative treatment protocol is identified that has improved effectiveness and is less likely to introduce collateral damage to the surrounding tissue. The alternative protocol uses 350 mW laser power with repeating laser tip movement to achieve bacterial disinfection in the deep dentin (800 μm lateral from the canal surface), while avoiding thermal damage to the surrounding tissue (T $<47°C$). The alternative treatment protocol has the potential to not only achieve bacterial disinfection of deep dentin but also shorten the treatment time, thereby minimizing potential patient discomfort during laser procedures. [DOI: 10.1115/1.3147801]

1 Introduction

Lasers have been used in dentistry for removing hard tooth tissue for more than 20 years [1]. In particular, the erbium, chromium: yttrium, scandium, gallium, garnet (Er,Cr:YSGG) laser with a wavelength of 2.78 μm is capable of achieving straight, clean, and precise hard tissue cuts [2–4]. Due to its long wavelength, the absorbed laser energy is limited within a very thin layer of the irradiated tissue and therefore, high temperature elevations ($>100°C$) at the surface result in hard tissue ablation.

Recently, lasers have also been proposed for use in root canal therapy for cleaning and for eliminating bacteria from the root canal system [5–7]. Currently, there are more than 40×10^6 root canal treatment procedures performed each year in the United States [8]. Root canal treatment aims to eliminate bacteria from the root canal system and to prevent spreading of infections to the head and neck region. Root canal bacteria, particularly Gram-positive facultative anaerobes, seem to be remarkably resistant to local antimicrobial agents that are often used in root canal therapy. In fact, cultivable bacteria were found in more than 40% cases [9–11]. Bacteria can also spread into the dentin tubules, where they may become protected from antimicrobial agents. It has been suggested that bacteria harbored in the tubules may contribute to persistent infections [12]. Nonthermal approaches to eliminate bacteria in endodontic treatments include sodium hypochlorite irrigation and photodynamic therapy [5]. Routine sodium hypochlorite irrigation may remove the majority (98%) of the bacteria within the canal but may not be very effective to bacteria located

within the deep dentin. Photodynamic therapy employs a photosensitizer that is activated by light, leading to formation of toxic oxygen species to damage cellular structures. This approach is also limited by light and the photosensitizer dye penetration to the deep dentin, as well as possible collateral photosensitivity accumulated in the periapical tissue. A recent in vitro study evaluated various preparation procedures for disinfecting the root canals using low-power laser with or without water spray [6]. The heat-induced cytotoxic response kills bacteria in the root dentin via heat conduction from the laser incident root canal surface [6]. The experimental studies were compared with that using sodium hypochlorite irrigation (the control). Wet laser treatments were less successful than sodium hypochlorite no matter how long the heating duration. Dry laser treatment was more effective than the control but only with a high power laser (350 mW) and a long period of heating (>60 s) [6].

There are several unanswered questions in laser treatment protocols considered for root canal therapy. One regards the heat penetration into the tissue. Previous experimental data have demonstrated that bacterial infection can spread through dentinal tubules as far as 800 μm lateral from the canal surface [12,13]. Although a pulsed laser can induce very high temperature elevations on the canal surface, it is unclear whether sufficient temperatures can be achieved in the deep dentin. In the in vitro study reported by Gordon et al. [6], the laser probe was moved up and down along a 5 mm root canal at a rate of 1 mm/s, since the affected region of the laser probe is limited to approximately 1 mm in the axial direction. After the probe was moved away from the canal surface segment, the temperature decayed back to the normal tissue temperature ($37°C$). As such it is still unknown whether the elevated temperature is sustained long enough in both the canal surface and deep dentin to fully kill bacteria.

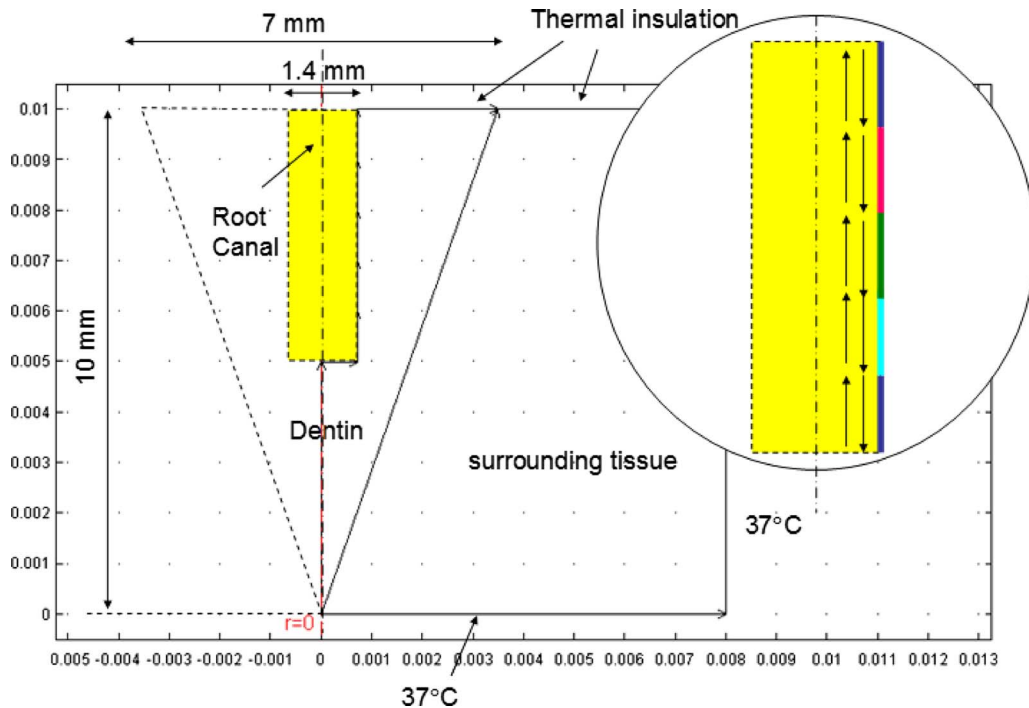A desired heat penetration can always be achieved using a high

Fig. 1 Schematic diagram of the axisymmetrical geometry of the tooth root and surrounding tissue. Laser tip is moved up and down in the canal and the heating time at each cylindrical segment is 1 s [6].

laser power and/or a long heating duration. However, the collateral damage to the tissue surrounding the tooth root is another issue that cannot be ignored. Previous in vitro studies using heating (System B HeatSource, Analytic Technologics, Redmond, WA) have illustrated a temperature elevation of more than $10°C$ on the outside surface of tooth root during heating procedures in the root canal [14,15]. Recent clinical practice involves utilizing pulsed rather than continuous laser energy to minimize heat transport from the irradiated surface to the outside surface of tooth root. In laser-assisted bacterial disinfection, one has to balance temperature elevation in the deep dentin and the thermal damage to the surrounding tissue. To our knowledge, there has been no theoretical study on the temperature distribution in root dentin arising from laser treatment, including an assessment of temperature elevations at the periodontal ligament and within the surrounding bony structure.

In this study, we develop a heat transfer model to estimate the temperature elevations in both the tooth root and surrounding tissue during Er,Cr:YSGG laser disinfection of the root canal surface. The laser power level, pulse setting, and laser duration are incorporated into the Pennes bioheat equation for the theoretical study. We first simulate the temperature distributions in the tooth root to evaluate whether heat penetrates into the deep dentin when using two published treatment protocols [6]. Based on the simulated results, we propose an alternative treatment protocol that achieves better heat penetration with shorter treatment time.

2 Mathematical Formulation and Methods

The tooth root and surrounding tissues are modeled as an axisymmetric structure, as shown in Fig. 1. We only consider a single-rooted tooth in this study as the first step. The root is surrounded by a body of tissue large enough that the temperature at the boundary surface is $37°C$. The adopted root canal geometry is modeled after that described in Ref. [6]. In that study, the root canal was prepared as a cylindrical cavity with an approximate canal volume of 8 μl and a root section of 5 mm in length. In the present study, we consider a root of 10 mm length and 7 mm

diameter. The average size of the root canal is 1.4 mm in diameter and 5 mm long to have the same canal volume as in Ref. [6]. Note that a prepared root canal is typically tapered toward the apex and 10–15 mm long. However, the goal of this study is to compare the simulated results with those from a previously reported in vitro study [6]. Hence, it is important to use a precise geometry consistent with that in the in vitro study.

Due to its long wavelength and a very large absorption coefficient of 10^4 cm^{-1}, we assume that the laser wave will not penetrate into the tooth root [16,17]. In this study its thermal effect is modeled as a uniform heat flux incident on the canal surface. The laser used in Ref. [6] is manufactured by Biolase Technology (YSGG Waterlase MD™, Biolase Technology, Irvine, CA). The current end-firing design only allows a limited emission range of approximately 1 mm in the axial direction. Since the laser has an affected region of approximately 1 mm in the axial direction [6], the laser tip was traversed in the canal in a cervical-apical and apical-cervical direction at a rate of 1 mm/s. This heating cycle requires 10 s to traverse the entire canal once (Fig. 1). In this study, we simulate the laser flux to follow the same time course, i.e., the heat flux stays in the 1-mm-long cylindrical segment for 1 s before it is moved to the next cylindrical segment.

The Er,Cr:YSGG laser is pulsed with a duration of 200 μs and a repetition rate of 20 pulses/s (20 Hz). In Ref. [6] the laser power was either 175 mW or 350 mW, which is equivalent to a power of 43.75 W or 87.5 W, respectively, during the pulse. The corresponding heat flux on the irradiated cylindrical canal segment is either 9.95×10^6 W/m^2 or 1.99×10^7 W/m^2 during the pulse (Fig. 2). Although the duration of the laser treatment varied from 15 s to 240 s in the in vitro study [6], a simulation duration of 10 s was chosen in the present study. Collateral tissue damage, defined as a temperature elevation higher than $47°C$ for more than 10 s, is assessed in all the treatment protocols [18].

We use the Pennes bioheat equation to simulate the heat transport in the tissue regions [19]. Neglecting metabolism, one can write it as
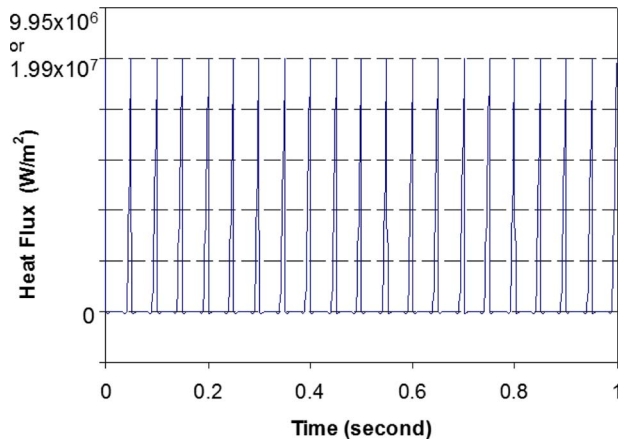
Fig. 2 Heat flux imposed to each cylindrical canal surface induced by the pulsed laser
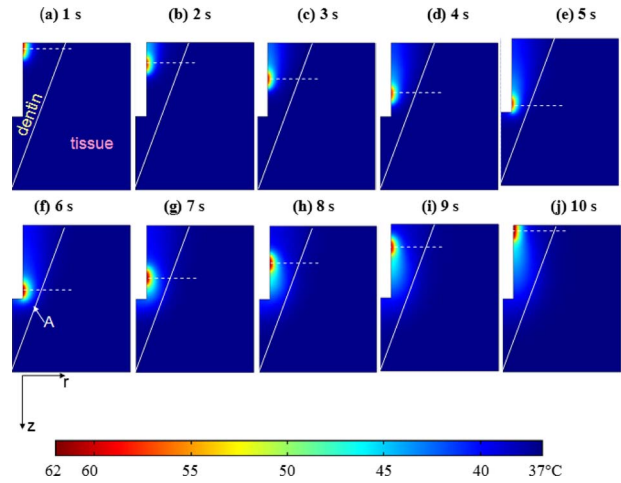

Fig. 3 Temperature contours of the root dentin and surrounding tissue during laser treatment using 175 mW, and the simulation time is 10 s. The white solid line represents the root-tissue interface. The closest location along the interface to the root canal wall is marked by "A."

$$\rho C \frac{\partial T_{\text{root,tissue}}}{\partial t} = k_{\text{root,tissue}} \nabla^2 T_{\text{root,tissue}} + \omega \rho_b C_b (37 - T_{\text{root,tissue}})$$

(1)

where k is the thermal conductivity, ρ is the density, C is the specific heat, and ω is the local blood perfusion rate. This equation is a modification of the traditional heat conduction equation with a heat source term. The thermal effect of the blood perfusion in the surrounding tissue is modeled as a heat source term with strength proportional to the local blood perfusion rate, and the temperature difference between the body temperature (37°C) and the local tissue temperature. Table 1 lists the thermal properties used in the simulation based on previous studies [20–22]. In root dentin the blood perfusion rate is zero, while in the surrounding tissue it is 1.8 ml/100 g/min [21]. The initial condition is 37°C in the entire domain.

All the finite element calculations including the mesh generation are performed using COMSOL® 3.3 operated on a Pentium IV processor of 2.79 GHz speed, using 2 Gbyte of memory under a Windows XP SP2 Professional operating system. The total number of tetrahedral elements of the finite element method is around 11375. The element growth rate and mesh curvature are selected as 1.2. A mesh convergence study was performed by increasing the number of elements in the dentin by 100% over the current mesh. The finer mesh induced less than 1% difference in the temperature field. The numerical model for heat transport is introduced by applying the Galerkin formulation of Eq. (1). We use a time-dependent solver known as UMFPACK. The time step is selected as 10^{-4} s and is half of the laser pulse duration.

3 Results

3.1 Temperature Fields Induced by 175 mW Laser. Since the heat flux is imposed on each segment for only 1 s, first we examine the temperature distribution on the individual segments over the canal depth. Temperature contours in the root dentin are presented in Fig. 3, where each image represents the temperature distribution after the 1 s heating. When the laser pulse energy setting is 175 mW, a temperature up to 57°C is achieved on the

canal surface and there is almost no temperature elevation on the other four segments. The surface temperature in treatment at segment 5 is higher than that in the other segments, since the heating time is 2 s rather than 1 s. Note that once the laser tip is moved up toward the crown, the temperatures in the other segments have returned to 37°C. Again, only a very mild increase in temperature is achieved. Table 2 lists the average temperature in the entire volume of the dentin at the end of each second. The average temperature change for one transverse of the laser tip is less than 3.3°C, indicating that heat conduction is not sustained after 1 s heating, especially when the laser power is low (175 mW).

The degree of heat penetration into the deep dentin is shown in Fig. 4; the radial temperature distributions in this figure correspond to that along the white dashed lines in Fig. 3. As shown in Fig. 4, temperature rises at distances of 200 μm, 400 μm, 600 μm, and 800 μm from the canal surface during the first 5 s are 52°C, 45°C, 41°C, and 39°C, respectively. When the laser tip is moved up toward the crown in the second 5 s period, the radial temperature distribution is 3°C higher than when the tip is moved down. Yet, the temperature at 800 μm in depth is still lower than 43°C. If bacteria penetrated the deep dentin, the rise in temperature would not be sufficient to kill all the bacteria.

3.2 Temperature Fields Induced by 350 mW Laser. We also simulated the temperature fields of the dentin using a 350 mW laser; all the parameters are the same except the heat flux imposed on the canal surface. Figure 5 compares the temperatures at five radial distances using both 175 mW and 350 mW. Note that

Table 1 Thermal properties used in the model

	k (W/m K)	ρ (kg/m³)	C (J/kg K)	ω (ml/min/100 g)
Root	0.57	2140	1400	0.0
Tissue	1.16	1500	2300	1.8

Table 2 Average dentin temperature as a function of time

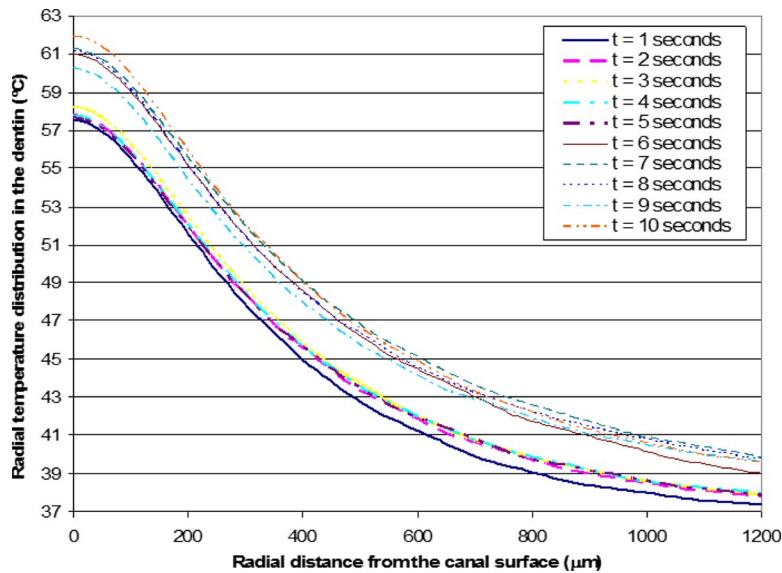| Time	175 mW (°C)	350 mW (°C)
1	37.5	38.0
2	37.9	38.9
3	38.4	39.9
4	38.8	40.7
5	39.2	41.4
6	39.4	41.9
7	39.6	42.3
8	39.8	42.7
9	40.0	43.1
10	40.3	43.6

Fig. 4 Radial temperature distribution along the white dashed lines shown in Fig. 3 during laser treatment using a laser power of 175 mW. Note that the temperature distribution represents that at various time instants.

there is a 100% increase in temperature using 350 mW at all locations. The maximum temperature at the surface reached 85°C, and the temperatures at 200 μm, 400 μm, 600 μm, and 800 μm lateral from the canal wall are 73°C, 60°C, 52°C, and 47°C, respectively.

Since the temperature gradient is much higher than that resulting from the previous protocol, it indicated that heat conduction through the dentin is enhanced when 350 mW is used. Table 2 lists the average temperature of the dentin induced by 350 mW heating. There is more than 6.6°C increase after heating for 10 s using 350 mW. If the 10 s heating protocol was repeated, one would see a greater temperature elevation in the later heating cycles, due to the accumulated heat remaining in the dentin. Thus, it is not surprising that bacterial killing was significantly improved in the experimental study [6], when the heating was prolonged.

Thermal damage may occur in the surrounding tissue. Figure 6 illustrates the temperature distribution along the root surface (along the white line in Fig. 3) at $t=6$ s, when the maximum temperature is likely to occur. As shown in Fig. 6, the maximum temperature is found at location A (Fig. 3), which is the closest to the root surface along the interface. However, the temperature is only increased up to 41°C, implying no thermal damage will be induced to the surrounding tissue using the protocols previously reported.

3.3 A New Alternative Protocol. Based on the simulated results in Secs. 3.1 and 3.2, it is evident that 175 mW is not sufficient to kill all bacteria in deep dentin, that heating duration of 1 s is unable to increase the temperature in the deep dentin above 47°C even at 350 mW, and that 350 mW will not induce thermal damage to the dentin-tissue interface if heating at each segment lasts less than 2 s. That implies that the protocol should be modified for improving the temperature distribution and killing bacteria. We will propose an alternative treatment protocol for laser disinfection of the root canal using 350 mW as the laser power level and a heating duration of 2 s at each cylindrical segment.
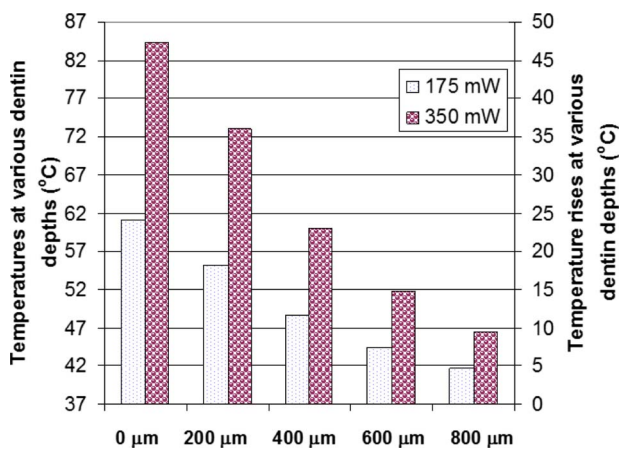

Fig. 5 Temperatures at various locations including the canal surface (0 mm) and in the deep dentin (200 μm, 400 μm, 600 μm, and 800 μm lateral from the canal surface) at $t=6$ s. The effect of the laser power is represented by different bars. The primary y axis on the left gives the actual temperature values, while the secondary y axis on the right illustrates the temperature elevations from the baseline of 37°C.
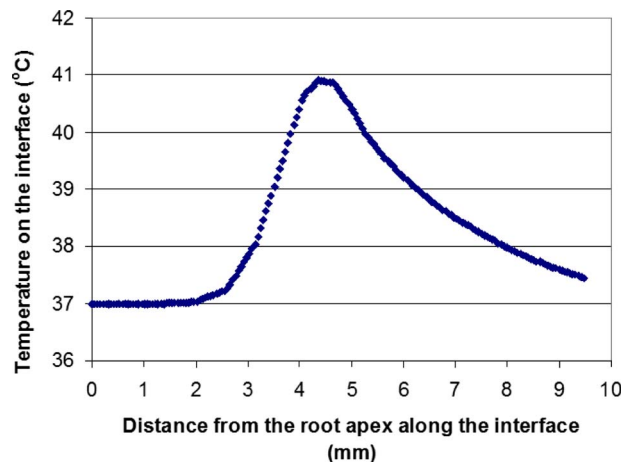

Fig. 6 Temperature profile along the root-tissue interface at $t=6$ s using the 350 mW laser. The white dashed line represents the dentin location with a radial offset of 800 μm from the root canal surface.
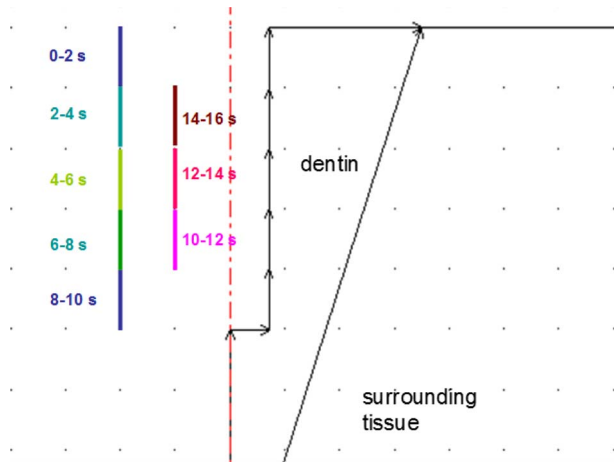
Fig. 7 Schematic diagram of the proposed treatment protocol. Different line segments represent different cylindrical surface segments of the root canal. Laser tip stays in each surface segment for 2 s, and the total time for each cycle is 16 s.

Fig. 9 Heat accumulation in the dentin during the first and second heating cycle (32 s) is illustrated by the average temperature of the entire dentin at various time instants

Here the laser tip is traversed along the canal in a cervical-apical and an apical-cervical direction in a discrete manner, which results in a transverse time (heating cycle) of 16 s, as shown in Fig. 7. The protocol is designed to achieve two objectives: (1) The temperature in deep dentin is elevated to at least 47°C for more than 10 s and (2) no thermal damage is induced to the dentin-tissue interface (<47°C). We also would like to identify the maximum heating duration to avoid thermal damage to the surrounding tissue. The simulation time is 32 s for two heating cycles.

Heat spreading from the root canal surface using the new protocol is shown in Fig. 8. Since the heating time for all segments is 2 s, the maximum temperature at the canal surface is increased to 93°C. Also note that the overall temperature field at $t=16$ s is significantly higher than that at $t=4$ s (Fig. 8). The average temperature of the entire dentin is calculated and presented in Fig. 9. Initially, the temperature increases at a rate of 1°C/s, then it slows down due to enhanced heat conduction in the tissue. Eventually, the total increase for the first heating cycle is around 9°C over 16 s or an average rate of 0.56°C/s. However, the average rate of the temperature increase during the second heating cycle decreases to 0.19°C/s. One may only see a minor temperature
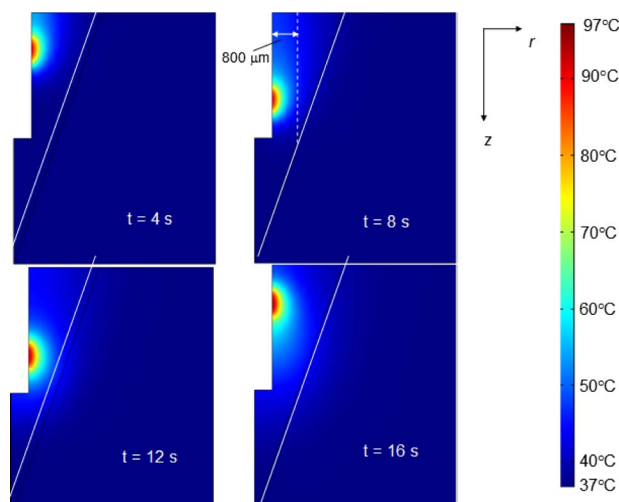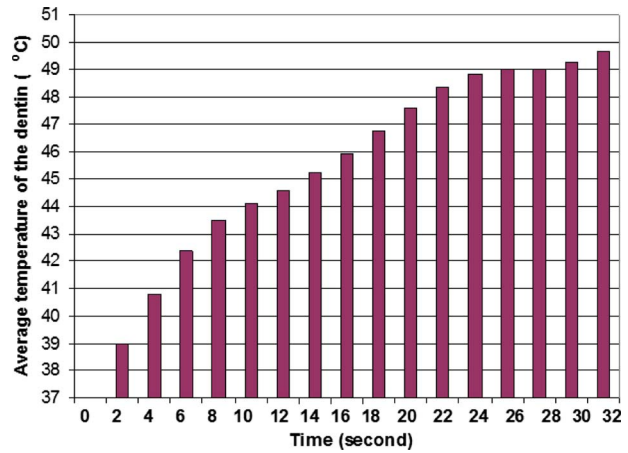
increase less than 0.19°C/s, if the heating cycle is further repeated, due to the thermal balance between heat conduction to the surrounding tissue and heat flux at the canal wall.

We are also interested in how heating affects the temperature distribution along the root canal surface. As shown in Fig. 10, temperature rise is significant at the location on which the laser energy is imposed. Initially, the temperature distribution along the canal surface at $t=2$ s is represented by the heavy solid line. When the laser tip moves to the next segment, the temperature profile is replaced by the next solid line. Note that the maximum temperature changes along the canal surface with the moving laser tip. For the same axial location (z), one observes that the temperature does not return to 37°C after the laser tip is moved away.

One of the major limitations of the previous protocol using 350 mW laser power is a failure to elevate the temperature of deep dentin to 47°C. In this study, we examine the temperature distribution along the white dashed line in Fig. 8. The line is parallel to the canal surface with a radial distance of 800 μm. Figures 11(a) and 11(b) illustrate the temperature profile along the 800 μm deep dentin region during the two heating cycles. For the same deep dentin location, its temperature, once it is elevated above 47°C, can be sustained after the laser tip is moved to the next

Fig. 8 Simulated temperature contours in the dentin and surrounding tissue using the proposed treatment protocol
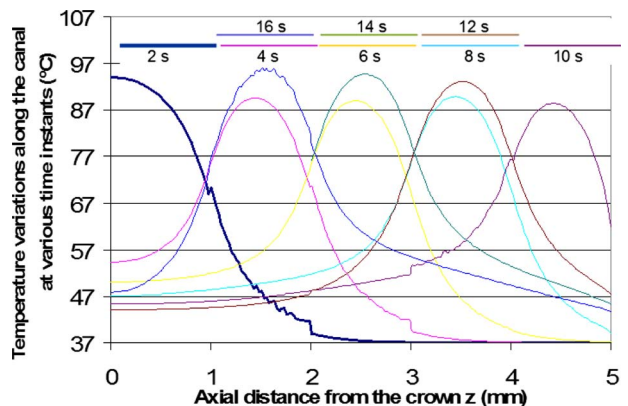

Fig. 10 Temperature profiles along the canal surface in the axial direction from the crown side. Initially the temperature distribution along the canal surface is represented by the heavy solid line. After the laser tip is moved to the next segment, the temperature distribution is replaced by the next solid line. Notice the shift of maximum temperature on the canal surface due to the fact that the laser tip is moved from one segment to another.
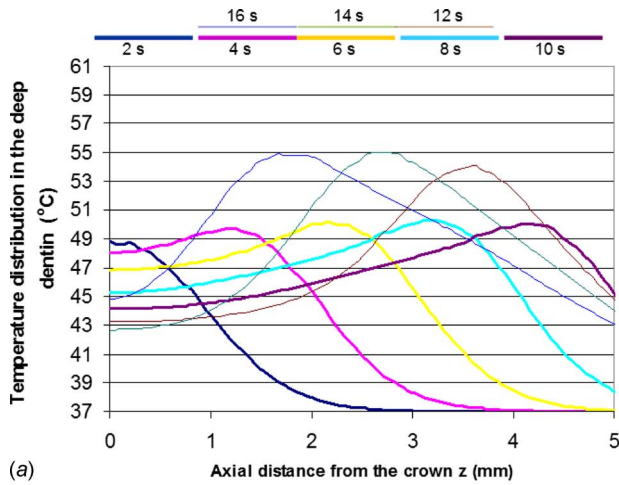
(a)
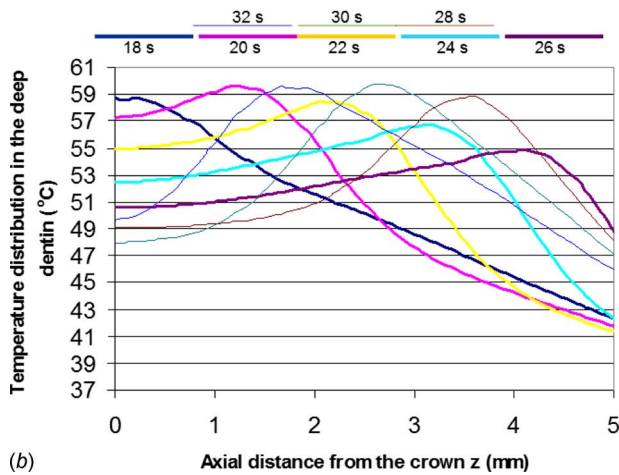
(b)

Fig. 11 Temperature distribution in the deep dentin (800 μm lateral from the canal surface, along the white dashed line in Fig. 8 at various time instants. Moving the laser tip up and down results in the shift of the maximum temperature. (a) The first heating cycle (0–16 s) and (b) the second heating cycle (16–32 s)
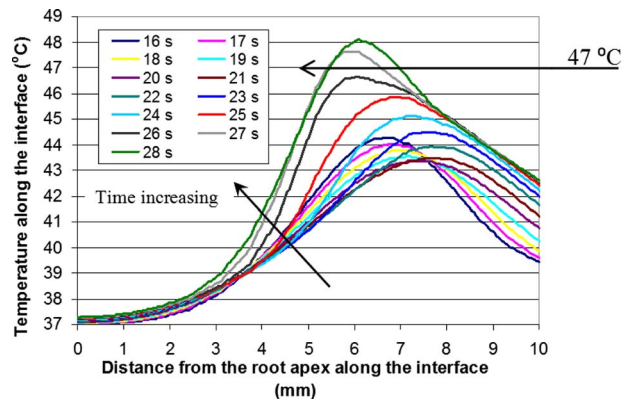

Fig. 12 Heat penetration from the canal surface to the soft tissue region is shown by the increasing temperature along the root-tissue interface with time. Temperatures are plotted along the root-tissue interface (the solid white line in Fig. 3) from the apex to the crown. The maximum temperature is lower than the critical temperature of 47°C when the heating time is shorter than 26 s.

canal segment. This is evident in the second heating cycle.

It is well known that the thermal-induced cytotoxic effect to bacteria depends not only on the temperature elevation but also on the heating duration. Our theoretical model can provide the entire temperature history at any location to estimate how long each dentin location is subject to a temperature of 47°C or higher. Table 3 gives the estimated time along the white dashed line in Fig. 8. Heating is not uniform in the deep dentin. As shown in

Table 3, after two heating cycles, the deep dentin in the middle segment is exposed to 47°C or higher for more than 23 s, while the minimal time is only 11 s. The exposure time decreases dramatically with the decrease in the heating time. The maximum exposure in deep dentin is merely 8 s after one heating cycle. Our results imply that to achieve bacterial eradication in deep dentin, the treatment protocol can be further improved to have a more uniform heat exposure.

Finally, thermal damage is assessed by the temperature rise along the interface between the dentin and surrounding tissue. As shown in Fig. 12, the interface temperature is lower than 45°C after the first heating cycle; however, it continues to increase during the second heating cycle. Usually location A is the most vulnerable location along the interface. However, due to heat conduction and the different laser heating segments, the maximum temperature location may shift slightly from location A. Our simulation suggests that the heating should not be longer than 26 s to avoid thermal damage to the surrounding tissue. As shown in Table 3, during a heating time of 26 s, the temperature in most of the deep dentin is elevated to 47°C or higher and maintained for more than 10 s.

4 Discussion

The mathematical simulation of the temperature field in the root dentin during laser disinfection is in good agreement with the results of the reported in vitro experiment [6]. Specifically, a laser power of 175 mW fails to elevate the deep dentin temperature above 42°C and the short heating time of 1 s is not long enough

Table 3 Total time for deep dentin subject to a temperature exceeding

| | Time when $T_{deep\ dentin} > 47°C$ | | | | |
| | Cervical → Apical | | | | |
Heating time (s)	Segment 1 (s)	Segment 2 (s)	Segment 3 (s)	Segment 4 (s)	Segment 5 (s)
4	1.4	0	0	0	0
8	1.7	1.1	2.2	0.6	0
12	1.7	1.1	3.7	4.6	2.2
16	1.8	3.0	7.5	8.6	3.8
20	5.6	7.0	11.5	10.3	3.8
24	9.6	11.0	15.5	12.9	4.0
28	13.6	15.0	19.5	16.9	7.6
32	17.6	19.0	23.5	20.9	11.4

to sustain any meaningful temperature rise. The theoretical simulation has demonstrated that repeating the same heating cycle may not be considerably more effective at killing bacteria with a low-power laser, even if the total heating is increased to as long as 240 s as shown in the in vitro experiments [6]; the bacterial survival rate still exceeded 2% at 175 mW for heating times from 15 s to 240 s. On the other hand, using a 350 mW laser power can result in higher temperatures in the entire dentin. Repeating the heating cycle may take advantage of the residual temperature rises from the previous heating cycles. However, due to the short heating time of 1 s, longer than 60 s are needed to expose the bacteria harboring in the deep dentin to 47°C or higher for sufficient time duration. Based on the limitations of the published protocols, a new protocol is proposed for the laser disinfection. The simulation has demonstrated the efficacy of employing a heating time of 2 s at each canal surface segment. It is determined that less than 26 s of treatment is required to prevent thermal damage to the surrounding tissue. Our model has illustrated that the proposed protocol enables most of the deep dentin to be exposed to temperatures exceeding 47°C for more than 10 s.

Bacteria harbored in the dentin are living organisms and should be subjected to biochemical events similar to tissue cells when exposed to heat. It is well known that heat-induced tissue damage depends on heating history, which includes both the tissue temperature and heating duration. Moritz and Henriques [23] originally assumed, which later became the standard for thermal injury evaluation, that the kinetics of the destruction process in living tissues is similar to the first order chemical reaction process, i.e., the Arrhenius integral. Results of the numerical simulation make it possible to assess the potential for thermal damage from the laser treatment once the coefficients in the Arrhenius integral are available. The dentin temperatures determined in the study $T(x,y,z,t)$ can be substituted into the Arrhenius integral to assess the degree of thermal damage. Unfortunately, the coefficients needed are unavailable for the evaluation. It is unclear whether the coefficients are the same between tissue cells and bacteria, and whether the coefficients change at different temperature ranges [24]. In this study, we assume that exposing the bacteria to 47°C for more than 10 s can kill the bacteria in the dentin based on previous experiments [18]. However, more experimental studies in dentin are needed to further investigate the bacterial tolerance to heating.

Although in vitro experiments can be performed to measure the temperatures inside the root canal and outside the tooth root [14,15,25,26], the detailed temperature distribution inside the root dentin is still unknown. The heat must reach a temperature threshold to kill the bacteria to the extent of penetration from the canal. Surface irrigation of sodium hypochlorite may not be effective to eradicate bacteria that have penetrated in the deep dentin. Therefore, a treatment plan that permits deep heat penetration while minimizing collateral thermal damage to the surrounding tissue is desirable. Quantitative thermal modeling aids in identification of an optimal treatment protocol and, with appropriate constitutive input data, affords the opportunity for designing personalized therapeutic regimens. Theoretical modeling can provide dentists with powerful tools to improve the ability to deliver safe and effective laser therapy. The thickness of root dentin and the root canal size may be different from one patient to another and from one kind of tooth to another. A theoretical model can be used for designing an individual effective treatment plan and ensuring safety for patients. For example, in the current practice, the catheter is held by the dentist who controls how long the catheter stays at each canal segment. As seen in Table 3, temperature elevations in the deep dentin is not uniform. The theoretical model can be implemented to determine how long or at what rate the laser tip is moving along the canal wall such that the bacterial killing zone is up to 800 μm from the canal surface and is uniform in the axial direction. However, it may require additional technical support to design a scanning apparatus for controlling the motion of the laser catheter.

In laser disinfection treatment, heat spreads from the root canal surface and can be quantitatively described by the Fourier number (dimensionless time) as

$$Fo = \alpha t / L^2 \qquad (2)$$

where t is time, α is the thermal diffusivity of the dentin, and L represents the distance from the root canal surface. Depending on how deep the bacteria penetrate inside the dentin, this relationship suggests that when the distance is doubled, the heating time should be four times of the original duration. The same principle can be applied to collateral thermal damage to the surrounding tissue. As shown in the simulation, the most likely location along the interface to have thermal damage should be that closest to the canal surface. For realistic root canal procedures, the root canal extends to the root apex. As such, the interface surrounding the apex is the most vulnerable location to thermal damage due to the low dentin thickness. In vitro experimental studies have shown higher temperatures at the outside root surface in incisors than in canines [14,15], which would be expected due to the lower dentin thickness in the incisors.

There are several limitations to this study. Optical fluctuation is not considered in the model. Induced optical property changes by temperature and/or dehydration may occur during the heating process. We did not model possible water vaporization since temperature can be higher than 100°C. The laser energy is modeled as a uniform heat flux incident on the root canal wall segment. Although this assumption satisfies the overall energy delivered to the canal wall, the heat flux may not be uniform due to the end-firing design of the laser catheter and beam divergence. In addition, laser induced temperature distribution on the wall may be more accurate than the uniform heat flux proposed in this study.

As we mentioned earlier, the proposed geometry of the root canal is simply a replica of that used in a previously reported in vitro experiment for comparing results. In reality the root canal is tapered and it extends to the root apex. One notes that the heat flux incident on the canal surface is directly related to the laser power as well as the canal surface area. For different root canal preparations, it would be interesting to investigate how the heat flux affects the canal surface temperature and the heat penetration. Another limitation is the thermal properties used in the model. As shown in Eq. (2), the thermal diffusivity α, which is defined as $k/\rho C$, also plays a role in determining the spreading of heat in the dentin. One notes that heat transfer rate is directly proportional to the thermal conductivity of dentin. Therefore, the accuracy of those properties can directly affect the simulation results [27] in thermal procedures. Unlike other tissues, there are limited publications in the literature on the thermal properties of the human dentin and the published data vary over a large range. Furthermore, an aged tooth root may have different microstructure (tubule size) than a young root, which may result in unique thermal properties [28,29]. Future theoretical simulations are needed to study how heat spreads from the canal surface to the deep dentin based on more realistic root geometry and tissue structure. Nevertheless, we still feel that the current model has provided insight in the fundamental physics that governs heat transport in this system. In fact, agreement between the theoretical prediction and experimental observation leads credibility to the current study.

5 Conclusions

A theoretical simulation employing the Pennes bioheat equation was used to understand how heat distributes in the tooth root during laser disinfection. The mathematical model is capable of determining heat penetration within the deep dentin during bacterial disinfection and assessing the potential for thermal damage to the surrounding vital tissue. Based on the simulated results, a treatment protocol has been identified that sustains adequate temperature elevation ($\geq$47°C) in the deep dentin for more than 10 s and utilizes a heating duration that precludes thermal damage to

the surrounding tissue. We believe that the proposed treatment protocol not only achieves thorough bacterial disinfection but also shortens the treatment time.

Acknowledgment

References

[1] Radatti, D. A., Baumgartner, J. C., and Marshall, J. G., 2006, "A Comparison of the Efficacy of Er,Cr:YSGG Laser and Rotary Instrumentation in Root Canal Debridement," J. Am. Dent. Assoc., **137**(9), pp. 1261–1266.

[2] Ishizaki, N., Matsumoto, K., Kimura, Y., Wang, X., Kinoshita, J., Okano, S., and Jayawardena, J., 2004, "Thermographical and Morphological Studies of Er,Cr:YSGG Laser Irradiation on Root Canal Walls," Photomed. Laser Surg., **22**(4), pp. 291–297.

[3] Matsuoka, E., Jayawardena, J. A., and Matsumoto, K., 2005, "Morphological Study of the Er,Cr:YSGG Laser for Root Canal Preparation in Mandibular Incisors With Curved Root Canals," Photomed. Laser Surg., **23**(5), pp. 480–484.

[4] Yamazaki, R., Goya, C., Yu, D., Kimura, Y., and Matsumoto, K., 2001, "Effects of Erbium, Chromium:YSGG Laser Irradiation on Root Canal Walls: A Scanning Electron Microscopic and Thermographic Study," J. Endod., **27**(1), pp. 9–12.

[5] Konopka, K., and Goslinski, T., 2007, "Photodynamic Therapy in Dentistry," J. Dent. Res., **86**(8), pp. 694–707.

[6] Gordon, W., Atabakhsh, V. A., Meza, F., Doms, A., Nissan, R., Rizoiu, I., and Stevens, R. H., 2007, "The Antimicrobial Efficacy of the Erbium, Chromium: Yttrium-Scandium-Gallium-Garnet Laser With Radial Emitting Tips on Root Canal Dentin Walls Infected With Enterococcus Faecalis," J. Am. Dent. Assoc., **138**(7), pp. 992–1002.

[7] Moritz, A., Jakolitsch, S., Goharkhay, K., Schoop, U., Kluger, W., Mallinger, R., Sperr, W., and Georgopoulos, A., 2000, "Morphologic Changes Correlating to Different Sensitivities of Escherichia Coli and Enterococcus Faecalis to Nd:YAG Laser Irradiation Through Dentin," Lasers Surg. Med., **26**, pp. 250–261.

[8] Bonavilla, J. D., Bush, M. A., Bush, P. J., and Pantera, E. A., 2008, "Identification of Incinerated Root Canal Filling Materials After Exposure to High Heat Incineration," J. Forensic Sci., **53**(2), pp. 412–418.

[9] Card, S. J., Sigurdsson, A., Orstavik, D., and Trope, M., 2002, "The Effectiveness of Increased Apical Enlargement in Reducing Intracanal Bacteria," J. Endod., **28**, pp. 779–783.

[10] Jha, D., Guerrero, A., Ngo, T., Helfer, A., and Hasselgren, G., 2006, "Inability of Laser and Rotary Instrumentation to Eliminate Root Canal Infection," J. Am. Dent. Assoc., **137**, pp. 67–70.

[11] Sjogren, U., Figdor, D., Persson, S., and Sundqvist, G., 1997, "Influence of Infection at the Time of Root Filling on the Outcome of Endodontic Treatment of Teeth With Apical Periodontitis," Int. Endod. J., **30**, pp. 297–306.

[12] Love, R. M., 2001, "Enterococcus Faecalis—A Mechanism for Its Role in Endodontic Failure," Int. Endod. J., **34**, pp. 399–405.

[13] Haapasalo, M., and Orstavik, D., 1987, "In Vitro Infection and Disinfection of Dentinal Tubules," J. Dent. Res., **66**(8), pp. 1375–1379.

[14] Lipski, M., 2005, "Root Surface Temperature Rises During Root Canal Obturation in Vitro by the Continuous Wave of Condensation Technique Using System B Heatsource," Oral Surg. Oral Med. Oral Pathol. Oral Radiol. Endod., **99**, pp. 505–510.

[15] Lipski, M., 2006, "In Vitro Infrared Thermographic Assessment of Root Surface Temperatures Generated by High-Temperature Thermoplasticized Injectable Gutta-Percha Obturation Technique," J. Endod., **32**, pp. 438–441.

[16] Aoki, A., Mizutani, K., Takasaki, A. A., Sasaki, K. M., Nagai, S., Schwarz, F., Yoshida, I., Eguro, T., Zeredo, J. L., and Izumi, Y., 2008, "Current Status of Clinical Laser Applications in Periodontal Therapy," Gen. Dent., **56**(7), pp. 674–687.

[17] Dederich, D. N., and Bushick, R. D., 2004, "Lasers in Dentistry: Separating Science From Hype," J. Am. Dent. Assoc., **135**, pp. 204–212.

[18] Eriksson, A. R., and Albrektsson, T., 1983, "Temperature Threshold Levels for Heat-Induced Bone Tissue Injury: A Vital-Microscopic Study in the Rabbit," J. Prosthet. Dent., **50**, pp. 101–107.

[19] Pennes, H. H., 1948, "Analysis of Tissue and Arterial Blood Temperatures in the Resting Human Forearm," J. Appl. Physiol., **253**, pp. H869–H873.

[20] Craig, R. G., and Peyton, F. A., 1961, "Thermal Conductivity of Tooth Structure, Dental Cements, and Amalgam," J. Dent. Res., **40**(3), pp. 411–418.

[21] Diao, C., Zhu, L., and Wang, H., 2003, "Cooling and Rewarming for Brain Ischemia or Injury: Theoretical Analysis," Ann. Biomed. Eng., **31**, pp. 346–353.

[22] Jakubinek, M. B., and Samarasekera, C., 2006, "Elephant Ivory: A Low Thermal Conductivity, High Strength Nanocomposite," J. Mater. Res., **21**(1), pp. 287–292.

[23] Moritz, A. R., and Henriques, F. C., 1947, "The Relative Importance of Time and Surface Temperature in the Causation of Cutaneous Burns," Am. J. Pathol., **23**, pp. 695–720.

[24] Welch, A. J., Pearce, J. A., Diller, K. R., Yoon, G., and Cheong, W. F., 1989, "Heat Generation in Laser Irradiated Tissue," ASME J. Biomech. Eng., **111**, pp. 62–68.

[25] Behnia, A., and McDonald, N. J., 2001, "In Vitro Infrared Thermographic Assessment of Root Surface Temperatures Generated by the Thermafil Plus System," J. Endod., **27**(3), pp. 203–205.

[26] Floren, J. W., Weller, N., Pashley, D. H., and Kimbrough, W. F., 1999, "Changes in Root Surface Temperatures With In Vitro Use of the System B Heatsource," J. Endod., **25**, pp. 593–595.

[27] Karmani, S., 2006, "The Thermal Properties of Bone and the Effects of Surgical Intervention," Curr. Pract. Orthop. Surg., **20**(1), pp. 52–58.

[28] Ten Cate, A. R., 1998, *Oral Histology in Development Structure and Function*, 5th ed., Mosby, St. Louis.

[29] Arola, D., 2007, "Fracture and Aging in Dentin," *Dental Biomaterials: Imaging, Testing and Modeling*, R. Curtis and T. Watson, eds., Woodhead, Cambridge, UK.